## Original Article

# The activation of M$_3$ muscarinic receptor reverses liver injury via the Sp1/lncRNA Gm2199/miR-212 axis

Haiying Zhang[1,†], Yanan Gao[1,†], Bin Liu[3], Haobin Jin[4], Li Fan[4], Xirui Yang[4], Qiang Gao[4], Yi Yu[1], Yueping Guo[2,4,*], and Yan Liu[1,*]

[1]Key Laboratory of Tropical Translational Medicine of Ministry of Education, College of Pharmaceutical, Hainan Medical University, Haikou 571199, China, [2]Hainan Medical University First Affiliated Hospital of Department of Anesthesiology, Haikou 570102, China, [3]Institute of Traditional Chinese Medicine, Hainan Medical University, Haikou 571199, China, and [4]Department of Pharmacology, Harbin Medical University, Harbin 150081, China

*Correspondence address. Tel/Fax: +86-898-66892193; E-mail: liuyan_gyp@163.com (Y.L.) / Tel: +86-13796051710; E-mail: 13796051710@163.com (Y.G.)

### Abstract

Muscarinic acetylcholine receptors (MRs) play important roles in the regulation of hepatic fibrosis and the receptor agonists and antagonists can affect hepatocyte proliferation. However, little is known about the impact of M$_3$R subtypes and associated signaling pathways on liver injury. The aim of this study is to explore the function and mechanism of M$_3$R in the regulation of liver injury. We evaluate liver injury and detect the changes in related indexes, including alanine aminotransferase (ALT), aspartate aminotransferase (AST), hydroxyproline (HYP), and transforming growth factor-β1 (TGF-β1), after administration of an M$_3$R agonist. Western blot analysis and qRT-PCR show that the transcription factor Sp1 and long noncoding RNA (lncRNA) Gm2199 are also changed significantly. Rescue assay is performed to further confirm that M$_3$R contributes to the progression of hepatocyte proliferation through regulating Sp1 and Gm2199. The activated M$_3$R can specifically regulate Gm2199 by inhibiting the expression of Sp1. Meanwhile, Gm2199 directly regulates miR-212, and ERK is a potential target of miR-212. Collectively, these findings define a novel mechanism for activating M$_3$R to reverse liver injury, which affects hepatocyte proliferation through the Sp1/Gm 2199/miR-212/ERK axis.

**Key words** liver injury, M$_3$ muscarinic acetylcholine receptor (M$_3$R), transcription factor Sp1, lncRNA Gm2199, miR-212

## Introduction

Liver injury results from various liver-related diseases, such as excessive drinking, viral infections, radiation damage, and drug effects [1]. Persistent liver injury can further lead to large-scale damage to liver cells, liver fibrosis and irreversible cirrhosis, and even death. Further exploration of the mechanism of liver injury is particularly important for the treatment of related liver diseases.

Existing studies have demonstrated that the activation of muscarinic and nicotinic receptors can modulate hepatocyte functions, but the mechanisms underlying cholinergic regulation of liver injury are unclear [2]. Of the five muscarinic acetylcholine receptors (MRs) designated as M$_1$R–M$_5$R, M$_3$R is the subtype primarily expressed in human and rodent liver [3,4]. It has been reported that M$_3$R gene ablation augments azoxymethane (AOM)-induced murine liver injury. In addition, AOM-induced liver injury is robustly exacerbated in M$_3$R-deficient mice [5,6]. These observa-

tions provide a proof-of-principle that selectively stimulating M$_3$R activation to prevent or diminish liver injury is a therapeutic strategy worthy of further investigation [7].

Long noncoding RNAs (lncRNAs) are a class of endogenous RNA molecules longer than 200 nucleotides in length [8]. These newly recognized regulatory molecules can participate in many fundamental biological processes and pathophysiological events. Although some lncRNAs have been documented to participate in the development of liver injury [9,10], the possible roles of these noncoding RNAs (ncRNAs) and the M$_3$R of the liver have not been thus far revealed. In our pilot studies, we analyzed the microarray profiling of lncRNA expression in a mouse model of liver injury characterized by hepatic damage manifested by a diminished proliferation capacity of hepatocytes. A multitude of lncRNAs and microRNAs (miRNAs) are differentially expressed to significant levels. Among these, Gm2199 stands out as a unique lncRNA that

has the potential to impose impacts on the development of liver injury [11]. We therefore carry out this study to explore the role of this lncRNA in regulating liver injury and to decipher the underlying cellular and molecular mechanisms. Unlike lncRNAs, miRNAs are a group of endogenous, evolutionarily conserve non-protein-coding RNA molecules with a typical length of nucleotides [12]. lncRNAs and miRNAs can communicate with and co-regulate each other through competing for endogenous RNA (ceRNA) or natural miRNA sponges [13, 14]. In order to provide sufficient elucidation of the complicated ncRNA regulatory network in liver diseases, we screen out absorbed miR-212 from the miRNA pool based on the sequence characteristics of lncRNA Gm2199 and further analyze the relationship among the miRNAs screened out for functional verification.

Sp1 is a ubiquitous transcription factor belonging to the zinc finger transcription factor family and is closely related to GC-rich promoter sequences [15]. Sp1 can regulate the expression of many related factors in the liver such as TGF-β1, and then regulates the activation of hepatic stellate cells (HSCs), thereby regulating the occurrence and development of liver fibrosis [16]. Sp1 can also regulate the expression of related lncRNAs, such as the lncRNA CTBP1-AS2 expression in liver cancer [17]. However, whether Sp1 participates in liver injury by regulating the expression of Gm2199 has yet to be determined.

In this study, we demonstrate for the first time that activation of M$_3$R attenuates CCl$_4$-induced liver injury. The transcription factor Sp1 and lncRNA Gm2199 are involved in the M$_3$R-mediated liver injury, which may be an important and potential new mechanism for the treatment of liver injury.

## Materials and Methods
### Animals
Male ICR mice (4-week-old) were obtained from the Experimental Animal Center of Harbin Medical University (Harbin, China). All animals were fed under the same conditions, a 12/12 h light/dark cycle and common mouse food and water. Animal testing procedures were approved by the National Institutes of Health's Guide to the Care and Use of Laboratory Animals (NIH Publication No. 85-23, revised in 1996). At the same time, all animal experimental protocols were pre-approved by the Experimental Animal Ethics Committee of Harbin Medical University.

### Experimental grouping
The effect of pilocarpine (a selective M$_3$R agonist) and 4-DAMP (an M$_3$R antagonist) was investigated in a CCl$_4$-induced liver injury model. ICR mice ($n = 24$) were randomly divided into 4 groups ($n = 6$): control group, mice were treated with soybean oil alone; CCl$_4$ group, mice were intraperitoneally injected twice a week with CCl$_4$ (Sigma-Aldrich, Taufkirchen, Germany) at a dose of 2.5 mL/kg mixed with 20% (v/v) soybean oil, for 4 weeks; pilocarpine group, mice were treated with the same volume of CCl$_4$ for 4 weeks, then intraperitoneally administered with pilocarpine (MCE, New Jersey, USA) at a dose of 2.5 mL/kg daily for a total of 2 weeks; 4-DAMP group, mice were first treated with the same volume of CCl$_4$ for 4 weeks, then treated with 4-DAMP (Sigma-Aldrich, Taufkirchen, Germany) for 30 min at a dose of 1.25 mL/kg, then intraperitoneally administered with pilocarpine at a dose of 2.5 mL/kg daily for a total of 2 weeks.

### Liver histopathology
The livers removed from the mice were weighted, and then fixed in 4% paraformaldehyde for 48 h at room temperature. Then, tissues were paraffin-embedded and sectioned into 5-μm pieces, and the liver sections were stained with hematoxylin and eosin (H&E) and Masson's trichrome (KeyGEN BioTECH, Nanjing, China) using standard protocol for microscopic examination (BX61; Olympus, Tokyo, Japan). Morphology and pathology were analyzed by two independent pathologists under blinded conditions.

### Measurement of serum levels of ALT and AST
The blood collected from the right ventricle was stored at room temperature for 4 h, and centrifuged at 1187 $g$ for 10 min, and then the supernatant was separated. Serum levels of alanine aminotransferase (ALT) and aspartate aminotransferase (AST) were measured using the corresponding test kits (C009-2 and C010-2; NJBI, Nanjing, China) according to the manufacturer's instructions.

### Measurement of hepatic HYP level
After being washed with sterile phosphate buffered saline (PBS), fresh liver tissues were cut into 80–100 mg samples, dried, accurately weighed, and treated with 1 mL of hydrolyzing reagent provided with the Hydroxyproline (HYP) kit (A030-2; NJBI, Nanjing, China) at 95°C for 20 min. After the pH of the hydrolysate was adjusted to 6.0–6.8, ddH$_2$O was added to the hydrolysate of each sample to 10 mL. Then, 4 mL of the diluted hydrolysate was filled with 25 mg of activated carbon, mixed and centrifuged at 1616 $g$ for 10 min. Then, 1 mL of the supernatant was dissolved in ddH$_2$O or 5 μg/mL standard application solution, and then the reacting reagent provided with the HYP assay kit was added and incubated at room temperature and 60°C for 10 to 15 min. The reaction mixture was then centrifuged at 1616 $g$ for 10 min. Then 200 μL of the supernatant from each sample was dissolved in ddH$_2$O or 5 μg/mL standard application solution in a 96-well microplate, and the absorbance was measured at 550 nm with a Synergy HTX microplate reader (BioTek Instruments, Winooski, USA). The content of liver HYP is expressed as μg/mg wet liver.

### Cell culture and transfection
The mouse AML12 hepatocyte cell line was obtained from American Type Culture Collection (ATCC, Mannassas, USA) and cultured in Dulbecco's modified Eagle's medium with Nutrient Mixture F-12 (DMEM/F-12) ( Thermo Fisher Scientific, Waltham, USA) supplemented with 10% fetal bovine serum (FBS), 5 μg/mL human insulin, 5 μg/mL transferrin, 3 ng/mL selenium, 40 ng/mL dexamethasone, 100 U/mL penicillin, and 100 μg/mL streptomycin at 37°C with 5% CO$_2$.

Transfections of AML12 cells were carried out using the Lipofectamine 2000 agent (Invitrogen, Carlsbad, USA) following the manufacturer's protocols. miR-212 (mimic-miR-212; 5′-ACCUUGGCUAGACUCUCUCUCUCUACUTT-3′), anti-miR-212 (AMO-miR-212; 5′-AGUAAGCAGUCUGAGCCAAGGUTT-3′) and the negative control (NC; 5′-CUACGGCCAUUGACUUGUCUACUTT-3′) were provided by RiboBio (Guangzhou, China). The empty plasmid (si-NC; sense 5′-UUCUCCGAACGUGUCACGUTT-3′, antisense 5′-ACGUGACACGUUCGGAGAATT-3′) and the interference plasmid (si-Sp1; sense 5′-GCAACAUUAUUGCUGCUAUTT-3′, antisense 5′-AUAGCAGCAAUAAUGUUGCTT-3′) were transfected into cells using lipo2000 (Invitrogen) according to the manufacturer's instructions. Six hours later, the transfection medium was changed to culture medium supplemented with 10% FBS. After 48 h, AML12

cells were treated with 9 mM CCl$_4$ for 24 h at 37°C.

For overexpression of Gm2199, plasmid pEGFP-N1 (*Bgl*III/*Pst*I, N0253t; Shanghai Generay Biotech Co., Ltd, Shanghai, China) was conjugated with full-length Gm2199 DNA (pEGFP-N1–Gm2199). A pEGFP-N1 conjugated with nothing (pEGFP-N1 vector) was kept as a negative control. Cells were incubated in a six-well plate at a density of $1 \times 10^5$ cells per well and a 96-well plate at a density of $4 \times 10^3$ cells per well before transfection. After 24 h, pEGFP-N1–Gm2199 or pEGFP-N1 vector was transfected into cells using X-treme GENE HP DNA Transfection Reagent (11749800; Roche, Basel, Switzerland). All cells were collected after 24 h for the assessments.

## CCK8 assay

Cells were seeded at a density of $4 \times 10^3$ cells/well in 96-well plates 24 h after pretreatment. After incubation, 10 μL of CCK-8 reagent (Cell Counting Kit-8; Dojindo Laboratories, Tokyo, Japan) was added to each well according to the instructions. The optical density value (OD) was measured with a microplate reader (Infinite 200 PRO; Tecan, Männedorf, Switzerland) at a wavelength of 450 nm. Each group was set up in three wells, and each measurement was repeated at least three times.

## EdU staining

For *in vitro* detection, the cells were cultivated on slides at the density of $4 \times 10^4$ cells/slide. After different interferences, EdU staining and Hoechst 33342 staining were performed using the Cell-Light™ EdU Apollo®567 In Vitro Imaging Kit (C10310-3; RiboBio). The ratios of EdU-positive cells to total cells (Hoechst 33342-positive cells) were calculated.

## Measurement of ROS levels

The cells were cultured in 24-well plates and co-treated with CCl$_4$ (9 mM) and pilocarpine (180 μM) for 24 h at 37°C. On the basis of liver injury model, the 4-DAMP group was treated with 100 nM 4-DAMP for 30 min, and then treated with pilocarpine (180 μM) for 24 h. Finally, the cells were incubated with serum-free medium containing 10 μM DCFH-DA (Beyotime, Shanghai, China) for 30 min. The cells were then washed three times with serum-free medium and observed and imaged with the BX61 fluorescence microscope.

## Quantitative real-time PCR (qRT-PCR)

Total RNA was extracted from liver tissue or AML12 cells using TRIzol reagent (Invitrogen) according to the manufacturer's protocol. The quantity and quality of RNA were determined with NanoDrop ND-1000 (Thermo Fisher Scientific). cDNAs were synthesized using 0.5 mg of total RNA, oligo(dT)12–18 primers, and a ReverTra Ace quantitative real-time reverse-transcription PCR (qRT-PCR) RT kit (FSQ-101; Toyobo, Osaka, Japan) following the manufacturer's protocol. Gene expression was detected by qRT-PCR using the cDNAs, THUNDERBIRD SYBR qPCR mix reagents (QPS-201; Toyobo) and gene-specific oligonucleotide primers on an ABI 7500 fast real-time PCR system (Applied Biosystems, Foster City, USA). A total volume of 20 μL reaction mixture was subject to the following PCR conditions: 95°C, 30 s for initial denaturation, 35 cycles of 95°C for 5 s and 60°C for 34 s. Gene expressions in liver samples and cells were determined using the $2^{-\Delta\Delta CT}$ method. The expression level of *GAPDH* or *U6* was used to normalize the relative gene expressions. Primer sequences are listed in Table 1.

**Table 1. Sequence of primers used in qRT-PCR**

| Gene name | | Primer sequence (5′→3′) |
|---|---|---|
| *Sp1* | Forward | ATGAGACAGCAGGTGGAGAAGGAG |
| | Reverse | CGGAGATGTGAGGTCTTGCCATATAC |
| *Gm2199* | Forward | GCAGACTGGGCAGGAGAAGC |
| | Reverse | CACCTCAGCCATTGAACTCG |
| *ERK1* | Forward | TCCAAGGGCTACACCAAATC |
| | Reverse | AGGTAGTTTCGGGCCTTCAT |
| *ERK2* | Forward | CACCAACCATTGAGCAAATG |
| | Reverse | GTTCAGCAGGAGGTTGGAAG |
| *GAPDH* | Forward | GGTTGTCTCCTGCGACTTCA |
| | Reverse | TGGTCCAGGGTTTCTTACTCC |
| *α-SMA* | Forward | CTCTGCCTCTAGCACACAACT |
| | Reverse | CCAGGGCTACAAGTTAAGGGT |
| *Col1α1* | Forward | GATGACGTGCAATGCAATGAA |
| | Reverse | CCCTCGACTCCTACATCTTCTGA |
| *TGFβ1* | Forward | GCCTGAGTGGCTGTCTTTTGA |
| | Reverse | GCTGAATCGAAAGCCCTGTATT |
| *miR-212* | Forward | GCGGCTAACAGTCTCCAGTC |
| | Reverse | CAGCCACAAAAGAGCACAAT |
| *U6* | Forward | GCTTCGGCAGCACATATACTAAAAT |
| | Reverse | CGCTTCACGAATTTGCGTGTCAT |
| *miR-212* | RT primer | CCTGTTGTCTCCAGCCACAAAAGAGCACA ATATTTCAGGAGACAACAGGTGGCCGT |
| *U6* | RT primer | CGCTTCACGAATTTGCGTGTCAT |

## Western blot analysis

Cells were lysed and protein concentration was quantified using a protein assay kit (Beyotime, Shanghai, China). Ten micrograms of total proteins were separated by 12% SDS-PAGE and transferred onto a PVDF membrane (Millipore, Boston, USA). The membrane was blocked with TBST containing 5% skim milk for 2 h at room temperature and then incubated with rabbit polyclonal antibodies against Sp1 (1:1000, NBP2-20460; Novus Biologicals, Littleton, USA), ERK1/2 (1:1000, 4695S; Cell Signaling Technology, Boston, USA), p-ERK1/2 (1:1000, 4370S; Cell Signaling Technology) and GAPDH (1:1000, 14C10; Cell Signaling Technology) at 4°C overnight. After washing, the membrane was incubated with HRP-conjugated rabbit-anti-goat IgG (Cell Signaling Technology) for 2 h at room temperature. The signal of the protein band was detected using ECL reagent (29050; Engreen Biosystem, Beijing, China).

## Statistical analysis

All data except the pathological results are expressed as the mean ± SEM. Significant differences in data between two groups were determined by Student's *t*-test and differences between multiple groups were determined by one-way ANOVA using SPSS 17.0 (IBM, Armonk, USA). $P < 0.05$ was considered statistically significant.

## Results

### Protective effect of M₃R on CCl$_4$-induced liver injury in mice

We examined the effects of M₃R on histopathological changes in CCl$_4$-induced liver injury. H&E and Masson's trichrome staining
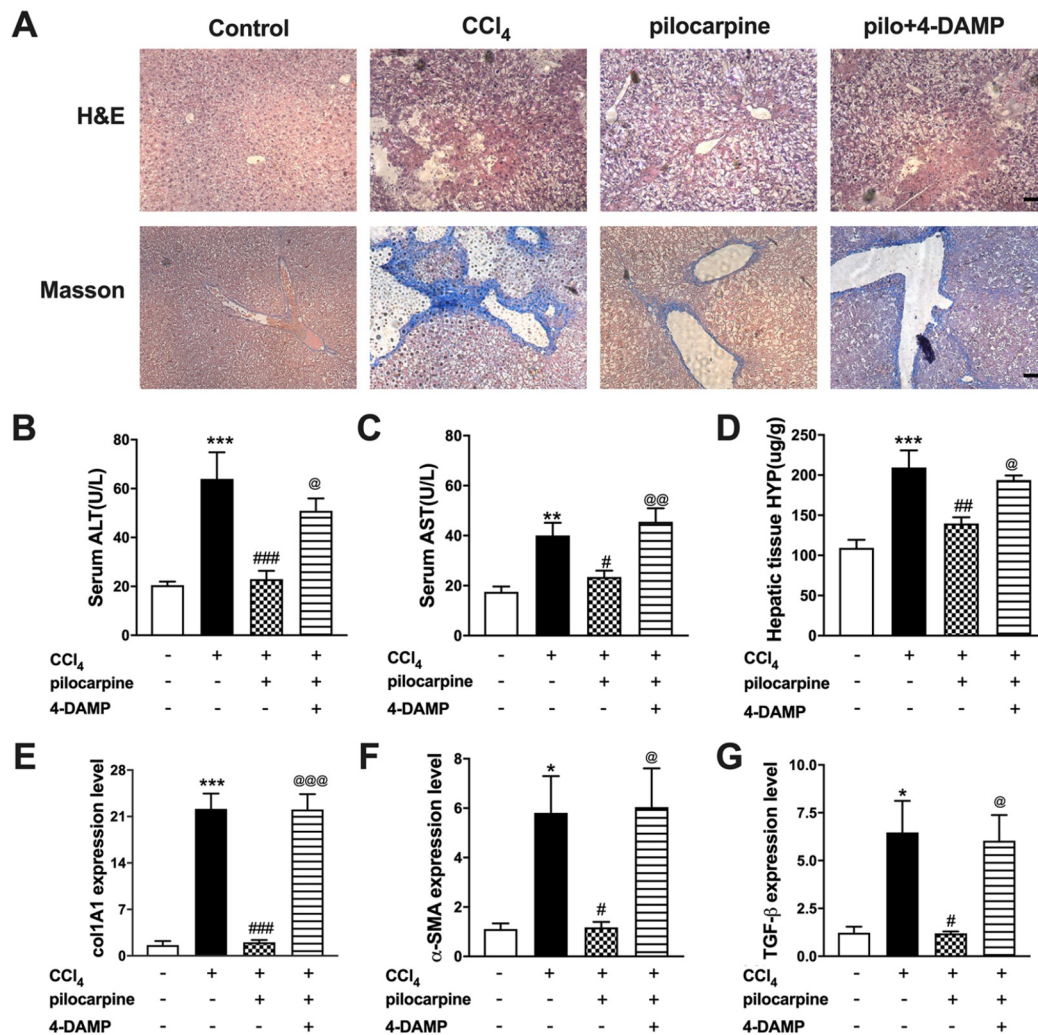
**Figure 1. Rescue effect of activating M$_3$R in damaged livers of mice** (A) External and histomorphological appearance of livers stained with hematoxylin and eosin and Masson's trichrome. Scale bar: 10 μm. (B–D) Serum ALT and AST contents and liver HYP level in mice. (E–G) qRT-PCR was used to detect the levels of liver injury-related genes including *Col1α1*, *α-SMA*, and *TGF-β1*. Data are expressed as the mean ± SEM (*n* = 3). *$P < 0.05$ and ***$P < 0.001$ vs control; #$P < 0.05$, ##$P < 0.01$ and ###$P < 0.001$ vs CCl$_4$; @$P < 0.05$, @@$P < 0.01$ and @@@$P < 0.001$ vs CCl$_4$ + pilocarpine.

revealed that the control livers had normal architecture with little fibrous portal expansion. Whereas, CCl$_4$-treated livers exhibited massive fatty changes, gross bridge necrosis, and broad infiltration of neutrophils and lymphocytes. CCl$_4$-treated livers also showed significant pericentral fibrosis with extensive blue-stained fibers. Compared with the model group, pilocarpine, the selective M$_3$R agonist, induced a significantly attenuated extent of liver injury. However, the attenuated effects of pilocarpine on liver injury were reversed by the M$_3$R antagonist 4-DAMP (Figure 1A). ELISA results showed that the levels of the hepatocyte injury markers ALT and AST in mouse serum were increased in the CCl$_4$-treated group compared with those in the control group. Pilocarpine treatment significantly inhibited ALT and AST levels, whereas pretreatment with 4-DAMP attenuated the effects of pilocarpine (Figure 1B,C). In addition, CCl$_4$ treatment increased the HYP content compared with the control group. Pilocarpine decreased the HYP content compared with the CCl$_4$ group, which was reversed by 4-DAMP (Figure 1D). We also found that the mRNA expressions of *Col1α1*, *α-SMA* and *TGF-β1*, which are fibrosis-related genes, were increased after the

incubation with CCl$_4$. However, their expressions in the pilocarpine-treated group were lower than those in the CCl$_4$ group, which was reversed by 4-DAMP treatment (Figure 1E–G). These results demonstrate that activation of M$_3$R has a protective effect on CCl$_4$-induced liver injury in mice.

### Activating M$_3$R relieves CCl$_4$-induced AML12 cell injury and promotes AML12 cell proliferation

Previous studies have demonstrated that ERK1/2 is closely related to cell proliferation [18]. Therefore, we postulated that ERK1/2 may mediate the effect of M$_3$R on the proliferation of injured hepatocytes. MTT assay was performed to determine the optimum concentration of pilocarpine in the treatment of AML12 cells. The survival rate of CCl$_4$-treated AML12 cells was increased when pilocarpine was administrated at 180 μM (Supplementary Figure S1). qRT-PCR and western blot analysis showed that ERK1 and ERK2 mRNA levels were significantly up-regulated after treatment with pilocarpine compared with the CCl$_4$ group, and the p-ERK protein level was also increased. Meanwhile, this phenotype was reversed by 4-DAMP.
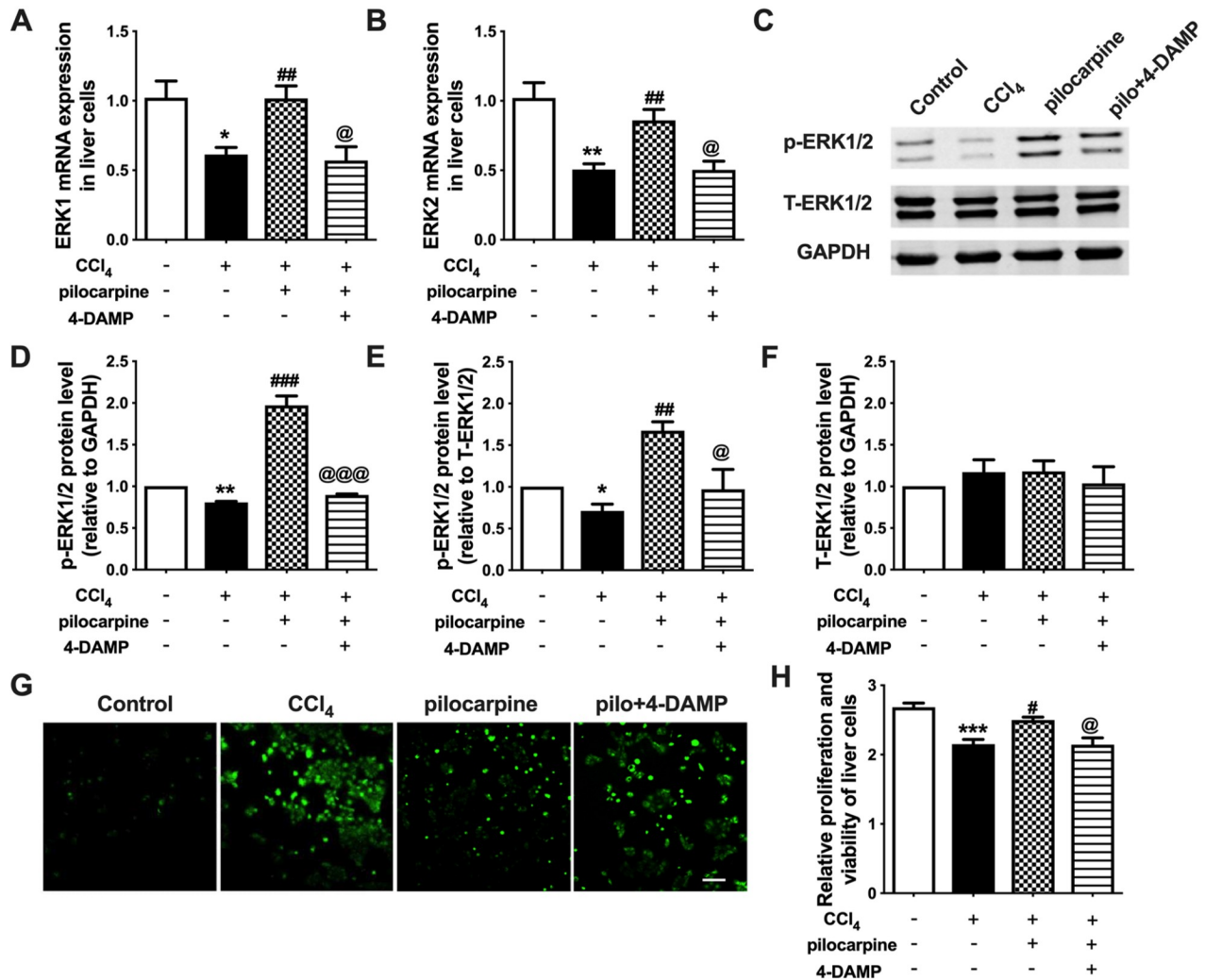
**Figure 2. Effects of activating M₃R on damaged hepatocytes and the expression of ERK1/2** (A,B) qRT-PCR analysis of ERK1 and ERK2 mRNA expressions in AML12 cells. (C–F) The protein expressions of p-ERK1/2 and T-ERK1/2 in AML12 cells with different treatments. (G) Production of intracellular ROS. Scale bars: 20 μm. (H) Cell proliferation was performed by CCK8 assay. Data are expressed as the mean ± SEM ($n = 3$). *$P < 0.05$, **$P < 0.01$ and ***$P < 0.001$ vs control; #$P < 0.05$, ##$P < 0.01$ and ###$P < 0.001$ vs CCl₄; @$P < 0.05$ and @@@$P < 0.001$ vs CCl₄ + pilocarpine.

However, there was no significant change in T-ERK1/2 protein levels between the groups (Figure 2A–F). It is possible that the regulation of M₃R affects protein translation. Nevertheless, the results indicate that activation of M₃R promotes phosphorylation of ERK1/2 and further leads to hepatocyte proliferation.

To further explore the role of M₃R *in vitro*, we evaluated the effect of M₃R on ROS production in the hepatocyte cell line AML12. The data indicated a significant increase in ROS production in CCl₄-treated AML12 cells (Figure 2G). However, pilocarpine treatment reduced CCl₄-induced intracellular ROS production, which was reversed by 4-DAMP. CCK8 assay results showed that after 24 h of pilocarpine treatment, the proliferation of AML12 cells was enhanced, which was reversed by 4-DAMP (Figure 2H). Therefore, these results indicate that the M₃R is involved in hepatocyte injury caused by CCl₄.

## Sp1 and Gm2199 are involved in M₃R-mediated protection against liver injury

To explore the function and mechanism of Gm2199 in M₃R-

mediated protection against liver injury, we measured Gm2199 expression in the liver and AML12 cells treated with CCl₄. In CCl₄-induced liver injury group, Gm2199 expression was significantly downregulated. Gm2199 was significantly upregulated in the CCl₄ + pilocarpine group in the liver and AML12 cells compared with that in the CCl₄ group. Interestingly, the effect of pilocarpine on Gm2199 was reversed by 4-DAMP (Figure 3A,B). Furthermore, we examined the mRNA and protein levels of the transcription factor Sp1. The expression of Sp1 was significantly increased in liver injury. Pilocarpine significantly downregulated CCl₄-induced upregulation of protein and mRNA levels of Sp1 in AML12 cells, which were reversed by 4-DAMP (Figure 3C,D). We also found that activation of M₃R decreased the expression of Sp1 in the nucleus (Supplementary Figure S2). Thus, M₃R activation might decrease the content of Sp1 in the nucleus, in addition to directly inhibiting its expression. From the above results, we know that Sp1 and Gm2199 are both involved in M₃R-mediated liver protection.
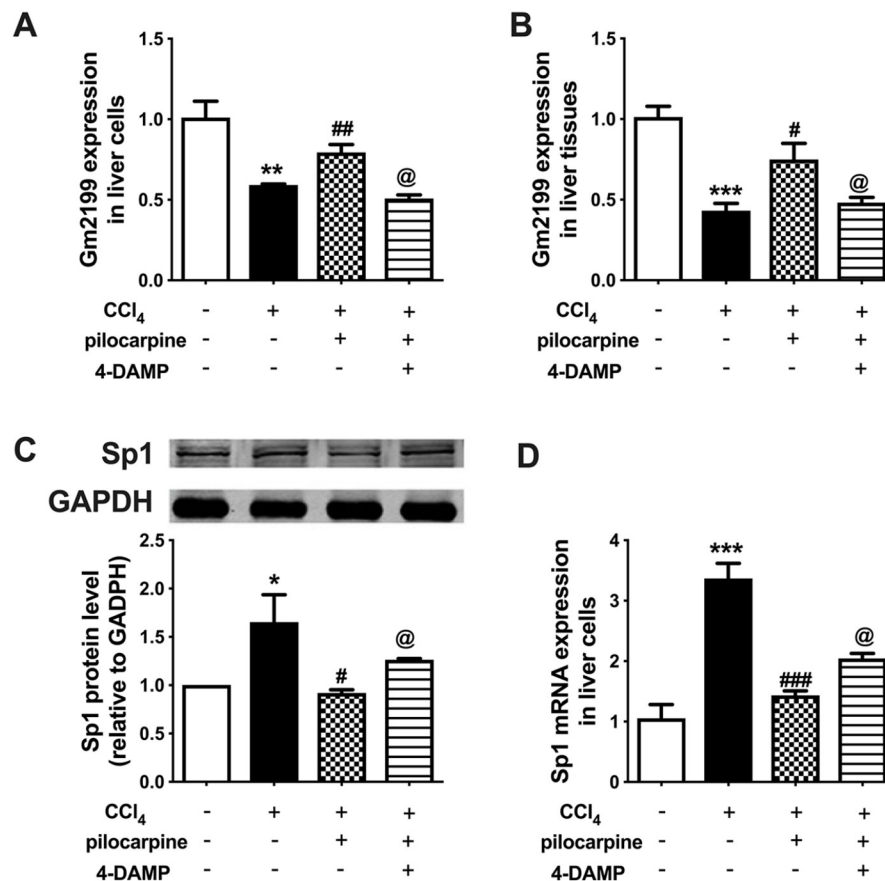
**Figure 3. Sp1 and Gm2199 are involved in M$_3$R-mediated liver protection** (A,B) qRT-PCR analysis of Gm2199 mRNA expression in AML12 cells and liver tissues. (C,D) Representative western blot analysis and qRT-PCR of Sp1 in AML12 cells. Data are expressed as the mean ± SEM ($n = 3$). *$P < 0.05$, **$P < 0.01$ and ***$P < 0.001$ vs control; #$P < 0.05$, ##$P < 0.01$ and ###$P < 0.001$ vs CCl$_4$; @$P < 0.05$ vs CCl$_4$ + pilocarpine.

## Sp1 may potentially regulate Gm2199

To further determine the relationship between Sp1 and Gm2199, the binding sites of Sp1 and Gm2199 promoter region were predicted using JASPAR (https://jaspar.genereg.net/search?advanced = -true). There were nine binding sites with a correlation score above 0.90 (Figure 4A). On this basis, we transfected si-Sp1 specifically into AML12 cells, and the transfection efficiency was satisfactory (Figure 4B). Moreover, Gm2199 expression was upregulated in liver cells after transfection with si-Sp1 compared with transfection with si-NC (Figure 4C). This indicates that Sp1 is likely to regulate Gm2199.

## Sp1 affects activation and expression of ERK1/2 in damaged AML12 cells

Our previous study revealed that Gm2199 can inhibit liver injury through the ERK1/2 pathway [11]. However, whether Sp1 is a key regulator in the up-regulation of ERK1/2 induced by M$_3$R activation needs further investigation. Therefore, to investigate the biological function of Sp1 in hepatocytes, we examined the expression of ERK1/2 by qRT-PCR and western blot analysis. The interference of si-Sp1 on protein expression was also successful. It was found that the protein expression of Sp1 was downregulated after transfection with si-Sp1 (Figure 5A,B). This is consistent with the change in mRNA expression in Figure 4B. Phosphorylated ERK1/2 (p-ERK1/2)

was significantly downregulated in CCl$_4$-induced hepatocyte injury compared with the normal group and total ERK1/2 (T-ERK1/2) protein expressions were unchanged. On this basis, p-ERK1/2 was upregulated in the CCl$_4$ + si-Sp1 group compared with in the CCl$_4$ + si-NC group, and there was no significant change in T-ERK1/2 (Figure 5C–F). Similarly, si-Sp1 reversed the down-regulation of ERK1 and ERK2 mRNAs in AML12 cells caused by CCl$_4$ (Figure 5G, H). CCK-8 assay revealed that CCl$_4$ treatment significantly inhibited cell proliferation, and the number of AML12 cells was 2-fold higher in the CCl$_4$ + si-Sp1 stimulation group than in the CCl$_4$ + si-NC stimulation group (Figure 5I). Therefore, these results indicate that transfection with si-Sp1 promotes the phosphorylation of ERK1/2 and further leads to hepatocyte proliferation, indicating that Sp1 is involved in liver injury caused by CCl$_4$.

## Identification of miR-212 as a target of Gm2199

It has been reported that many lncRNAs are ceRNAs for specific miRNAs. To examine whether Gm2199 exerts its function in liver injury as a ceRNA, we utilized the StarBase software (https://starbase.sysu.edu.cn/) and measured the miRNAs predicted to bind with Gm2199. As shown in Figure 6A, miR-212 was significantly negatively correlated with Gm2199 in liver injury. AML12 cells were transfected with pEGFP-N1–Gm2199, and it was found that Gm2199 overexpression resulted in the repression of miR-212 expression

**A**

| Matrix ID | Name | Score | Relative score | Sequence ID | Start | End | Strand | Predicted sequence |
|-----------|------|-------|----------------|-------------|-------|------|--------|--------------------|
| MA0079.2 | SP1 | 13.2935 | 0.966082163 | 5 | 453 | 462 | + | CCCCCCCCCC |
| MA0079.2 | SP1 | 12.3964 | 0.943489426 | 5 | 492 | 501 | + | CCCCACCCCC |
| MA0079.2 | SP1 | 12.1807 | 0.938058457 | 5 | 556 | 565 | − | CCCCTCCCTC |
| MA0079.2 | SP1 | 11.8365 | 0.92938962 | 5 | 1179 | 1188 | − | CCCCTCCCCT |
| MA0079.2 | SP1 | 11.3147 | 0.916248215 | 5 | 1180 | 1189 | − | CCCCCTCCCC |
| MA0079.2 | SP1 | 11.867 | 0.930156696 | 5 | 1182 | 1191 | − | CCCCCCCTCC |
| MA0079.2 | SP1 | 13.2935 | 0.966082163 | 5 | 1185 | 1194 | − | CCCCCCCCCC |
| MA0079.2 | SP1 | 11.9455 | 0.932135222 | 5 | 1378 | 1387 | − | CCCCTCCGCC |
| MA0079.2 | SP1 | 13.2935 | 0.966082163 | 5 | 1782 | 1791 | + | CCCCCCCCCC |
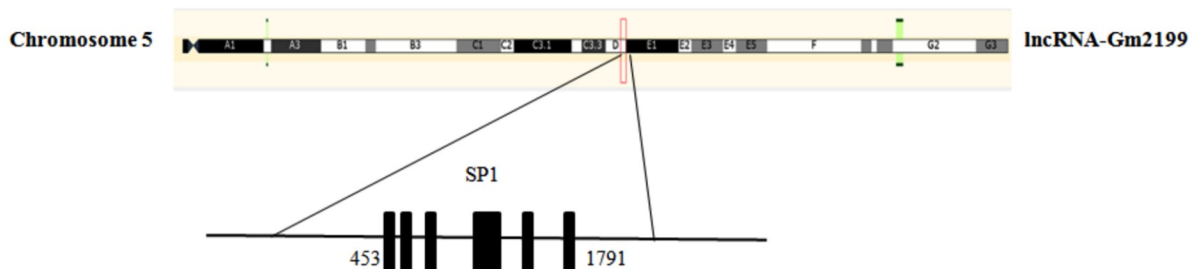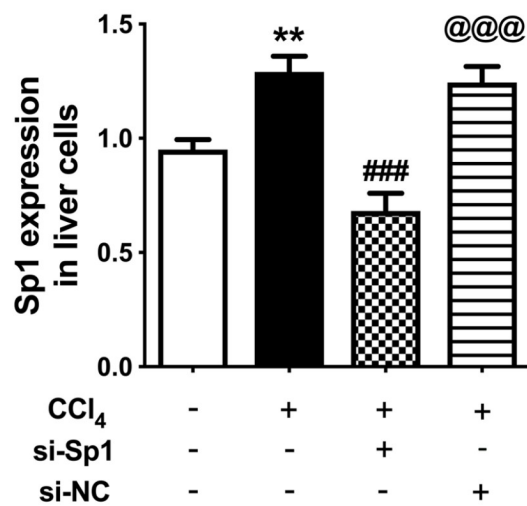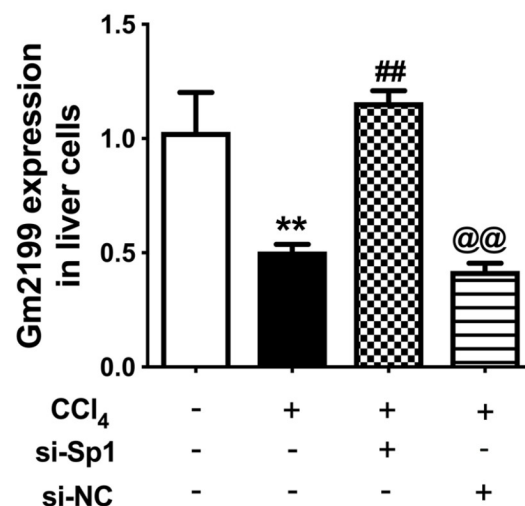


**Figure 4. The transcription factor Sp1 may potentially regulate Gm2199** (A) It is predicted by the Jaspar website that there is a binding site for the promoter of *Gm2199* and the transcription factor Sp1, and there are 9 sites with a correlation score above 0.9. (B) qRT-PCR was used to detect Sp1 mRNA expression in AML12 cells co-transfected with si-Sp1. (C) qRT-PCR analysis of Gm2199 mRNA of AML12 cells co-transfected with si-Sp1. Data are expressed as the mean ± SEM ($n = 3$). **$P < 0.01$ vs control; #$P < 0.05$ and ##$P < 0.01$ vs CCl₄; @@$P < 0.01$ and @@@$P < 0.001$ vs CCl₄ + si-

relative to the NC group, indicating that Gm2199 could directly sponge miR-212 (Figure 6A). To further verify the effect of miR-212 and its relationship with Gm2199 in liver injury, AMO-miR-212 was transfected into AML12 cells and its effects on cell proliferation were tested. CCK8 assay showed that AMO-miR-212 increased the proliferation activity of AML12 cells, while its mimic inhibited the cell proliferation activity, and this inhibitory effect could be offset by overexpression of Gm2199 (Figure 6B). The EdU staining assay result was consistent with that of CCK8 assay (Figure 6C). We further found that miR-212 is a potential ERK1/2 regulatory target through TargetScan software (https://www.targetscan.org/vert_80/) (Figure 6D). After successful transfection of mimic-miR-212, we detected the expression changes of p-ERK1/2 and T-ERK1/2 by western blot anlysis. Results in Figure 6E showed that miR-212 significantly reduced the level of p-ERK1/2 in AML12 cells compared with the control group. However, there was no significant difference in T-ERK1/2 between the two groups. qRT-PCR showed that the total mRNA levels of ERK1 and ERK2 were downregulated after transfection with mimic-miR-212, and AMO-miR-212 could reverse this phenomenon (Figure 6F). These results suggest that overexpression of miR-212 in normal AML12 cells inhibits cell proliferation and survival by reducing p-ERK1/2 levels. Thus, miR-212 might be involved in the function exerted by Gm2199 in M₃R-mediated protection against mouse liver injury.
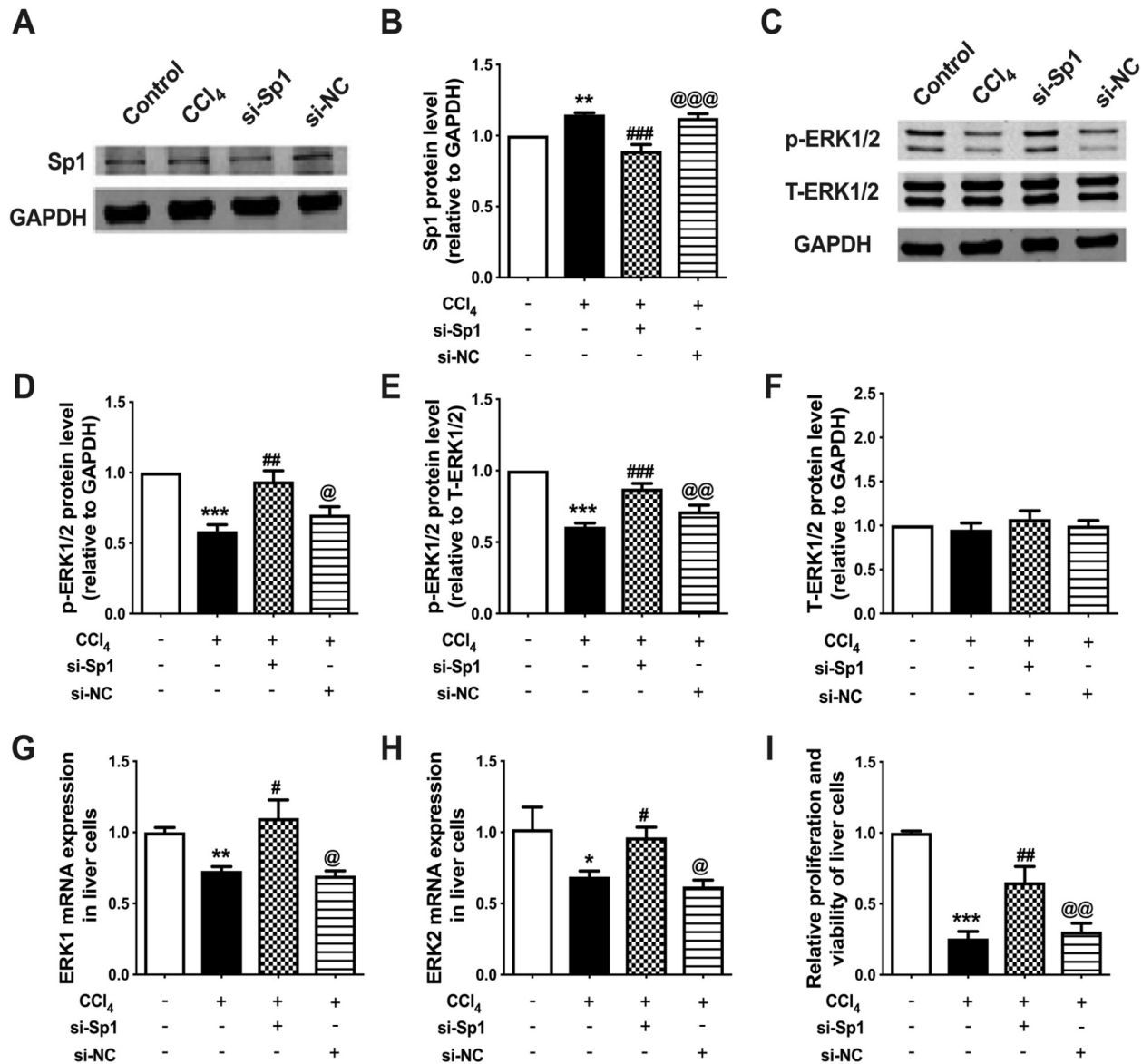
**Figure 5. Effect of si-Sp1 on activation of damaged hepatocytes and expression of ERK1/2** (A–F) Representative western blot analysis results of Sp1, p-ERK1/2 and T-ERK1/2 from control, CCl₄, CCl₄ + si-Sp1 and CCl₄ + si-NC treated AML12 cells. (G,H) qRT-PCR analysis of ERK1 and ERK2 mRNA expressions in AML12 cells. (I) Hepatocyte proliferation was detected by CCK8 assay. Data are expressed as the mean ± SEM (*n* = 3). \**P* < 0.05, \*\**P* < 0.01 and \*\*\**P* < 0.001 vs control; #*P* < 0.05, ##*P* < 0.01 and ###*P* < 0.001 vs CCl₄; @*P* < 0.05, @@*P* < 0.01 and @@@*P* < 0.001 vs CCl₄ + si-Sp1.

## Discussion

Liver injury, which has an extremely poor prognosis and high mortality, lacks effective therapies. In our previous study, we reported that Gm2199 is downregulated in CCl₄-induced liver injury in mice, whereas overexpression of Gm2199 promotes hepatocyte proliferation and alleviates liver injury [11]. In the present study, we found that activating M₃R has protective effects on CCl₄-induced liver injury in mice. Sp1 and Gm2199 are significantly altered during M₃R-mediated protection against liver injury, suggesting that Sp1 and Gm2199 may be involved in protecting the liver. Nevertheless, miR-212 in CCl₄-treated AML cells showed the opposite changes. In addition, we found that knockdown of miR-212 stimulates the MAPK signaling pathway activation. These results remind us of a

new possible mechanism by which M₃R protects the liver in CCl₄-induced liver injury.

It has been demonstrated that the muscarinic M₁ subtype is also involved in liver injury in mice. Substantial sequence homology among MR subtypes suggests that M₃Rs are also potential targets for regulating liver injury, however they demonstrate surprising individuality in their responses to stimuli [19–21]. In our study, we observed the effect of M₃R on CCl₄-induced liver injury. Many studies have shown that serum ALT, AST levels and HYP levels are significantly increased during liver injury, indirectly reflecting the degree of liver injury [22]. We found that treatment with CCl₄ significantly increased collagen fiber content and upregulated the expression of fibrosis-related genes such as *α-SMA*, *col1α1* and *TGF-*
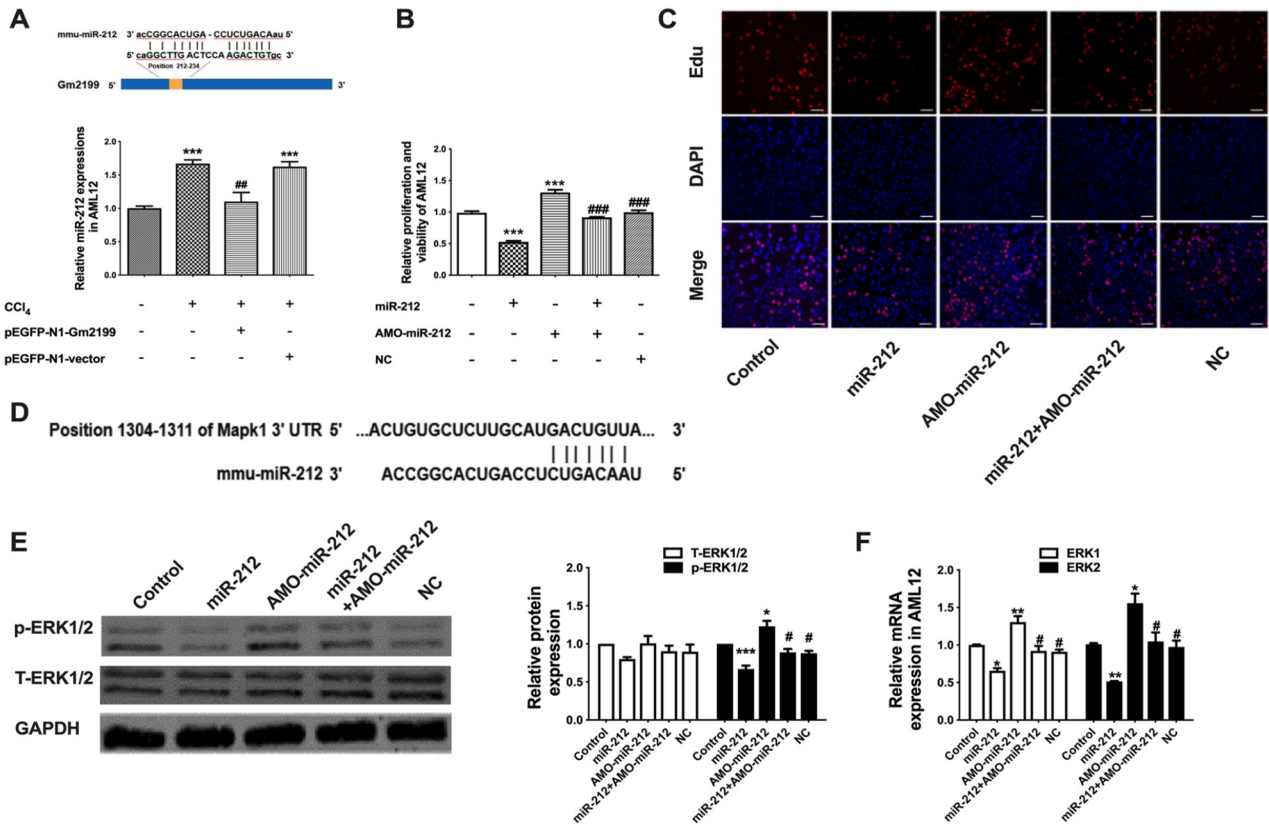
**Figure 6. Gm2199 serves as a sponge of miR-212 and ERK1/2 is a target of miR-212** (A) Bioinformatics analysis of the binding between Gm2199 and miR-212 was performed using Hybird. The expression of miR-212 in cells of each group was detected by qRT-PCR. (B,C) Cell proliferation was performed by CCK8 assay and EdU staining. Scale bars: 20 μm. (D) The putative binding region between ERK1/2 3′UTR and miR-212 was analyzed via TargetScan. (E) Protein expressions of p-ERK1/2 and T-ERK1/2 in each group of AML12 cells were analyzed by western blot analysis. (F) The expressions of ERK1 and ERK2 mRNA in each group of hepatocytes were analyzed by qRT-PCR. Data were expressed as the mean ± SEM ($n$ = 5). *$P$ < 0.05, **$P$ < 0.01 and ***$P$ < 0.001 vs control; #$P$ < 0.05 and ###$P$ < 0.001 vs AMO-miR-212.
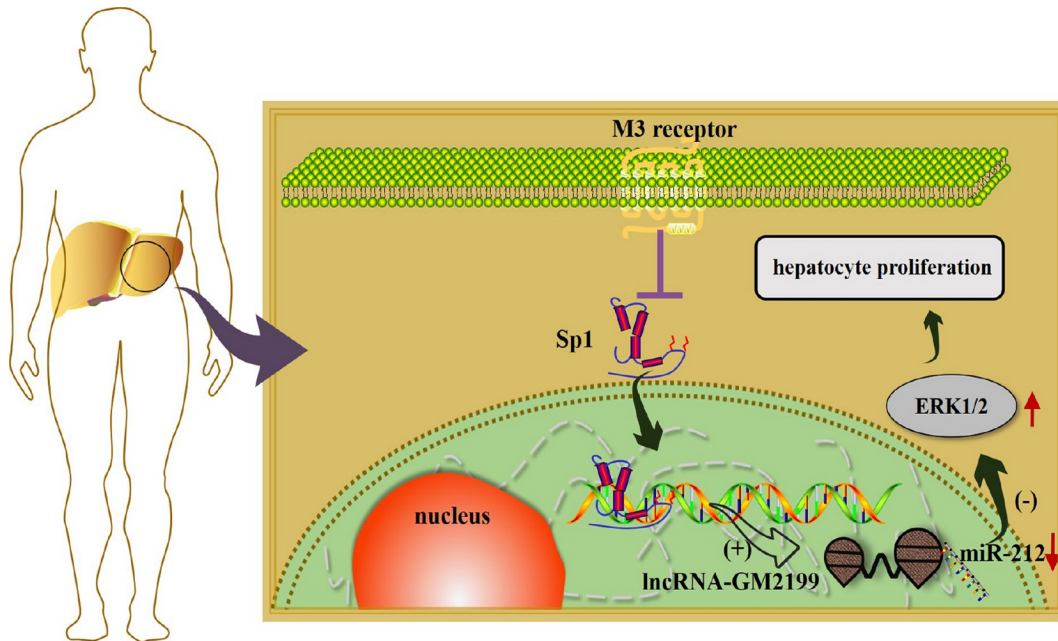


**Figure 7. Schematic diagram depicting the proposed signaling mechanisms underlying the effects of M$_3$R in the setting of liver injury** Activating M$_3$R can inhibit the expression and nuclear translocation of transcription factor Sp1, and then promote the expression of lncRNA Gm2199. Gm2199 can promote the expression of ERK1/2 and alleviate liver injury by inhibiting miR-212.

*β1*, while treatment with pilocarpine significantly reduced serum ALT and AST levels and liver HYP content in tissues. The M₃R antagonist 4-DAMP reversed these results. These data show that M₃R reduces CCl₄-induced liver injury by reducing fibrosis.

To further explore the possible mechanisms by which M₃R is activated to reduce liver injury, we focused on lncRNAs to investigate the role of lncRNAs in liver injury. Many studies have shown that lncRNAs are likely to be used as powerful diagnostic and prognostic indicators and even effective therapeutic targets in related liver diseases [9,23–25]. Although we have reported that overexpression of lncRNA Gm2199 can alleviate liver injury [11], the mechanism of Gm2199 in liver injury remains unexplored. In the present study, we found that treatment with pilocarpine significantly increased Gm2199 expression in CCl₄-induced liver injury, which could be reversed by 4-DAMP. Our results indicate that Gm2199 is involved in M₃R-mediated liver protection. miRNA is closely associated with the occurrence of liver diseases such as hepatitis, NAFLD, fibrosis, cirrhosis and HCC [26]. It has been revealed that lncRNAs function as ceRNAs, thereby releasing the miRNA-bound target genes [27–29]. Based on the interactive effect between miRNAs and lncRNAs, we screened out miR-212 which interacts with Gm2199.

The transcription factor Sp1 can regulate the expression of related lncRNAs, such as lncRNA HOTAIR and lncRNA CTBP1-AS2 in liver cancer [17,30]. Sp1 can also regulate the expressions of many related factors in the liver, such as TGF-β1, and then regulate the activation of HSCs. Therefore, Sp1 is becoming recognized as a key mediator in liver lesions. In the current study, we found that Sp1 is significantly elevated in the liver injury model, and after activation of M₃R, Sp1 expression is significantly downregulated. We also confirmed that Sp1 negatively regulates Gm2199 and exerts a certain influence on hepatocyte proliferation. These findings allowed us to draw up the following signaling pathway as a new mechanism for the long-recognized yet poorly understood in liver injury: activation of M₃R can specifically regulate Gm2199 by inhibiting the expression of Sp1; Gm2199 acts as a sponge of miR-212, which can promote the expression of ERK1/2 by inhibiting miR-212 (Figure 7). In conclusion, our results indicate that M₃R may serve as a novel therapeutic target for the treatment of liver injury.

## Supplementary Data

Supplementary data is available at *Acta Biochimica et Biphysica Sinica* online.

## Funding

## Conflict of Interest

The authors declare that they have no conflict of interest.

## References

1. Bessone F, Dirchwolf M, Rodil MA, Razori MV, Roma MG. Review article: drug-induced liver injury in the context of nonalcoholic fatty liver disease—a physiopathological and clinical integrated view. *Aliment Pharmacol Ther* 2018, 48: 892–913

2. Jadeja RN, Rachakonda VP, Khurana S. Targeting cholinergic system to modulate liver injury. *Curr Drug Targets* 2018, 19: 938–944

3. Jadeja RN, Chu X, Wood C, Bartoli M, Khurana S. M3 muscarinic receptor activation reduces hepatocyte lipid accumulation via CaMKKβ/AMPK pathway. *Biochem Pharmacol* 2019, 169: 113613

4. Luo L, Zhang G, Mao L, Wang P, Xi C, Shi G, Leavenworth JW. Group II muscarinic acetylcholine receptors attenuate hepatic injury via Nrf2/ARE pathway. *Toxicol Appl Pharmacol* 2020, 395: 114978

5. Luo L, Xi C, Xu T, Zhang G, Qun E, Zhang W. Muscarinic receptor mediated signaling pathways in hepatocytes from CCL4-induced liver fibrotic rat. *Eur J Pharmacol* 2017, 807: 109–116

6. Khurana S, Jadeja R, Twaddell W, Cheng K, Rachakonda V, Saxena N, Raufman JP. Effects of modulating M3 muscarinic receptor activity on azoxymethane-induced liver injury in mice. *Biochem Pharmacol* 2013, 86: 329–338

7. Durchschein F, Krones E, Pollheimer MJ, Zollner G, Wagner M, Raufman JP, Fickert P. Genetic loss of the muscarinic M₃ receptor markedly alters bile formation and cholestatic liver injury in mice. *Hepatol Res* 2018, 48: E68

8. Sarropoulos I, Marin R, Cardoso-Moreira M, Kaessmann H. Developmental dynamics of lncRNAs across mammalian organs and species. *Nature* 2019, 571: 510–514

9. Zhang CC, Niu F. LncRNA NEAT1 promotes inflammatory response in sepsis-induced liver injury via the Let-7a/TLR4 axis. *Int Immunopharmacol* 2019, 75: 105731

10. Chen J, Huang X, Wang W, Xie H, Li J, Hu Z, Zheng Z, *et al.* LncRNA CDKN2BAS predicts poor prognosis in patients with hepatocellular carcinoma and promotes metastasis via the miR-153-5p/ARHGAP18 signaling axis. *Aging* 2018, 10: 3371–3381

11. Gao Q, Gu Y, Jiang Y, Fan L, Wei Z, Jin H, Yang X, *et al.* Long non-coding RNA Gm2199 rescues liver injury and promotes hepatocyte proliferation through the upregulation of ERK1/2. *Cell Death Dis* 2018, 9: 602

12. Hücker SM, Fehlmann T, Werno C, Weidele K, Lüke F, Schlenska-Lange A, Klein CA, *et al.* Single-cell microRNA sequencing method comparison and application to cell lines and circulating lung tumor cells. *Nat Commun* 2021, 12: 4316

13. Zhang W, Tang G, Zhou S, Niu Y. LncRNA-miRNA interaction prediction through sequence-derived linear neighborhood propagation method with information combination. *BMC Genomics* 2019, 20: 946

14. Beermann J, Piccoli MT, Viereck J, Thum T. Non-coding RNAs in development and disease: background, mechanisms, and therapeutic approaches. *Physiol Rev* 2016, 96: 1297–1325

15. Ma WG, Shi SM, Chen L, Lou G, Feng XL. SP1-induced lncRNA FOXD3-AS1 contributes to tumorigenesis of cervical cancer by modulating the miR-296-5p/HMGA1 pathway. *J Cell Biochem* 2021, 122: 235–248

16. Zhang KF, Wang J, Guo J, Huang YY, Huang TR. Metformin enhances radiosensitivity in hepatocellular carcinoma by inhibition of specificity protein 1 and epithelial-to-mesenchymal transition. *J Can Res Ther* 2019, 15: 1603–1610

17. Liu LX, Liu B, Yu J, Zhang DY, Shi JH, Liang P. SP1-induced upregulation of lncRNA CTBP1-AS2 accelerates the hepatocellular carcinoma tumorigenesis through targeting CEP55 via sponging miR-195-5p. *Biochem Biophys Res Commun* 2020, 533: 779–785

18. Tomasovic A, Brand T, Schanbacher C, Kramer S, Hümmert MW, Godoy P, Schmidt-Heck W, *et al.* Interference with ERK-dimerization at the nucleocytosolic interface targets pathological ERK1/2 signaling without cardiotoxic side-effects. *Nat Commun* 2020, 11: 1733

19. Khan SM, Min A, Gora S, Houranieh GM, Campden R, Robitaille M, Trieu P, *et al.* Gβ4γ1 as a modulator of M3 muscarinic receptor signalling and novel roles of Gβ1 subunits in the modulation of cellular signalling. *Cell Signal* 2015, 27: 1597–1608

20. Mahati E, Li P, Kurata Y, Maharani N, Ikeda N, Sakata S, Ogura K, *et al.*

M3 muscarinic receptor signaling stabilizes a novel mutant human ether-a-go-go-related gene channel protein via phosphorylation of heat shock factor 1 in transfected cells. *Circ J* 2016, 80: 2443–2452

21. Rachakonda V, Jadeja RN, Urrunaga NH, Shah N, Ahmad D, Cheng K, Twaddell WS, *et al.* M1 muscarinic receptor deficiency attenuates azoxymethane-induced chronic liver injury in mice. *Sci Rep* 2015, 5: 14110

22. Chiu YJ, Chou SC, Chiu CS, Kao CP, Wu KC, Chen CJ, Tsai JC, *et al.* Hepatoprotective effect of the ethanol extract of Polygonum orientale on carbon tetrachloride-induced acute liver injury in mice. *J Food Drug Anal* 2018, 26: 369–379

23. Wang BG, Lv Z, Ding HX, Fang XX, Wen J, Xu Q, Yuan Y. The association of lncRNA-HULC polymorphisms with hepatocellular cancer risk and prognosis. *Gene* 2018, 670: 148–154

24. He Z, Yang D, Fan X, Zhang M, Li Y, Gu X, Yang M. The roles and mechanisms of lncRNAs in liver fibrosis. *Int J Mol Sci* 2020, 21: 1482

25. Chao Y, Zhou D. lncRNA-D16366 is a potential biomarker for diagnosis and prognosis of hepatocellular carcinoma. *Med Sci Monit* 2019, 25: 6581–6586

26. Kweon M, Kim JY, Jun JH, Kim GJ. Research trends in the efficacy of stem cell therapy for hepatic diseases based on microRNA profiling. *Int J Mol Sci* 2021, 22: 239

27. Lei H, Gao Y, Xu X. LncRNA TUG1 influences papillary thyroid cancer cell proliferation, migration and EMT formation through targeting miR-145. *Acta Biochim Biophys Sin* 2017, 49: 588–597

28. Zhao C, Qiu Y, Zhou S, Liu S, Zhang W, Niu Y. Graph embedding ensemble methods based on the heterogeneous network for lncRNA-miRNA interaction prediction. *BMC Genomics* 2020, 21: 867

29. Xu JH, Chang WH, Fu HW, Yuan T, Chen P. The mRNA, miRNA and lncRNA networks in hepatocellular carcinoma: an integrative transcriptomic analysis from Gene Expression Omnibus. *Mol Med Report* 2018, 17: 6472

30. Ren F, Ren JH, Song CL, Tan M, Yu HB, Zhou YJ, Qin YP, *et al.* LncRNA HOTAIR modulates hepatitis B virus transcription and replication by enhancing SP1 transcription factor. *Clin Sci* 2020, 134: 3007–3022